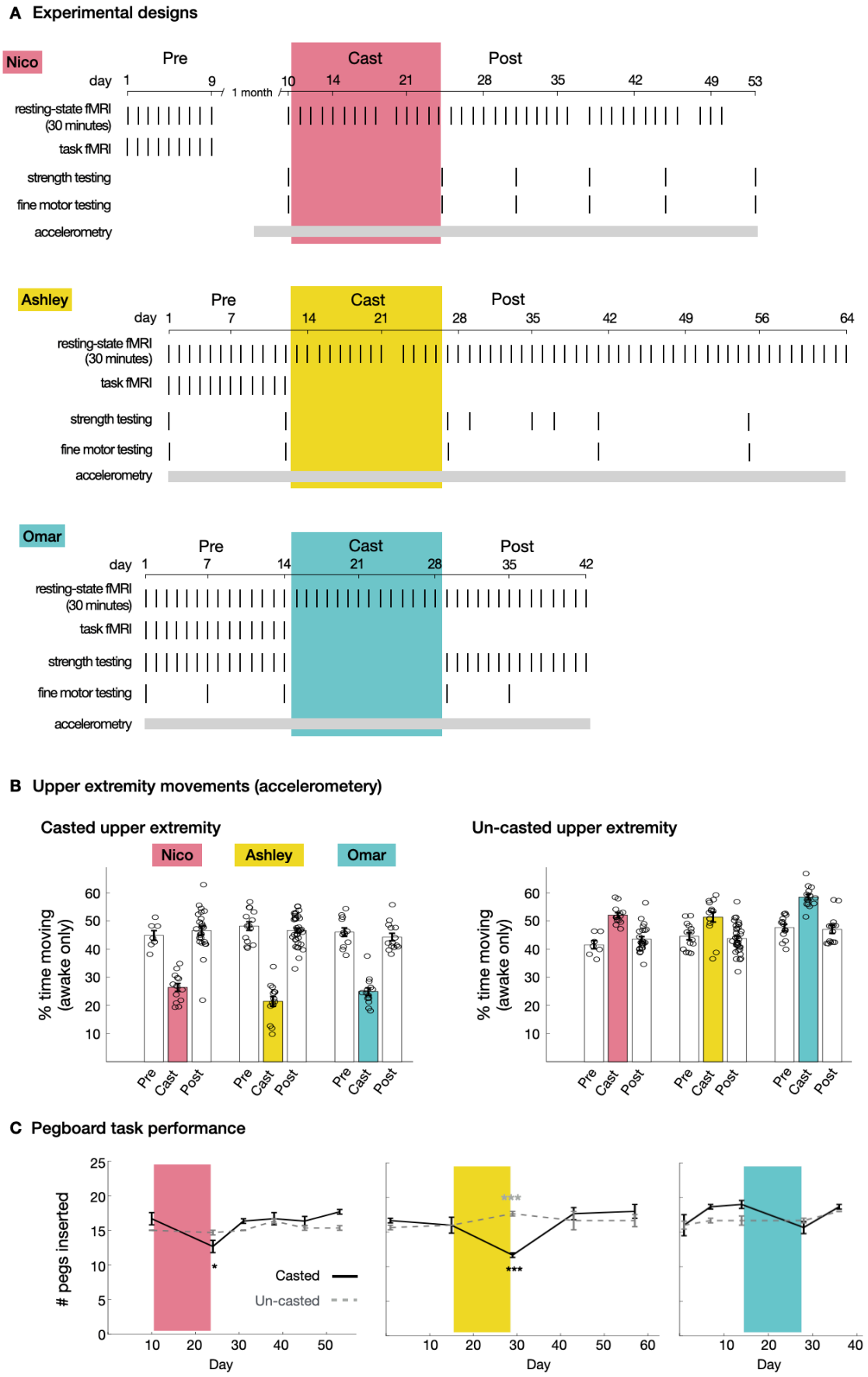

Figure S1: See next page for caption.

Figure S1: Casting induced changes in upper extremity use and fine motor skills, related to Figure 1. (A) Experimental design for all participants. Data acquisition included resting-state functional MRI (rs-fMRI), task-based functional MRI (fMRI), strength testing, fine motor testing, and continuous behavioral monitoring using wearable accelerometers. MRI sessions were missed only for unresolvable technical reasons, e.g., scanner not available. The principal investigator of the study, a 35-year-old male ('Nico'), served as a pilot participant. He was scanned 35 out of 38 consecutive mornings at 5:00 a.m. using a Siemens Trio 3T MRI scanner. Baseline data consisted of 1 session acquired immediately before casting and 9 sessions acquired using an identical protocol one month before casting. Our second participant, a 25-year-old female ('Ashley'), was scanned 63 out of 64 consecutive nights at 9:00 p.m. using a Siemens Prisma 3T MRI scanner. Baseline data consisted of 12 sessions acquired immediately prior to casting. Our third participant, a 27-year-old male ('Omar'), was scanned 42 out of 42 consecutive nights at 9:00 p.m. using the same scanner and MRI acquisition sequences that were used for Ashley (Supplementary Table 1). Baseline data consisted of 14 scans acquired immediately prior to casting. (B) *Left:* Upper extremity movements during daily activity were monitored using accelerometers worn on each wrist for the full duration of the experiment. Daily use counts were computed as the number of seconds during each day during which movement was detected. Use counts were normalized by the total time awake each day to yield % time moving. Bars show average use counts during each experimental period (Pre, Cast, Post) ± s.e.m. All participants used the casted upper extremity significantly less during the cast period (Nico: -41%, $P < 0.001$; Ashley: -55%, $P < 0.001$; Omar: -46%, $P < 0.001$). *Right:* All participants used the un-casted upper extremity significantly more during the cast period (Nico: +25%, $P < 0.001$; Ashley: +15%, $P = 0.004$; Omar: +23%, $P < 0.001$). (C) Fine motor skill was assessed using the Purdue pegboard task. Error bars indicate ± s.e.m. across three task runs. Immediately after cast removal, two participants showed significantly reduced performance of the casted extremity (# pegs inserted in 30 seconds) and one participant showed a trend in the same direction (Nico: -24%, $P = 0.033$; Ashley: -29%, $P < 0.001$; Omar: -12%, $P = 0.12$). One participant showed significantly increased performance of the un-casted extremity and two participants did not show any significant change (Nico: -2%, $P = 0.37$; Ashley: +11%, $P < 0.001$; Omar: +1%, $P = 0.70$).

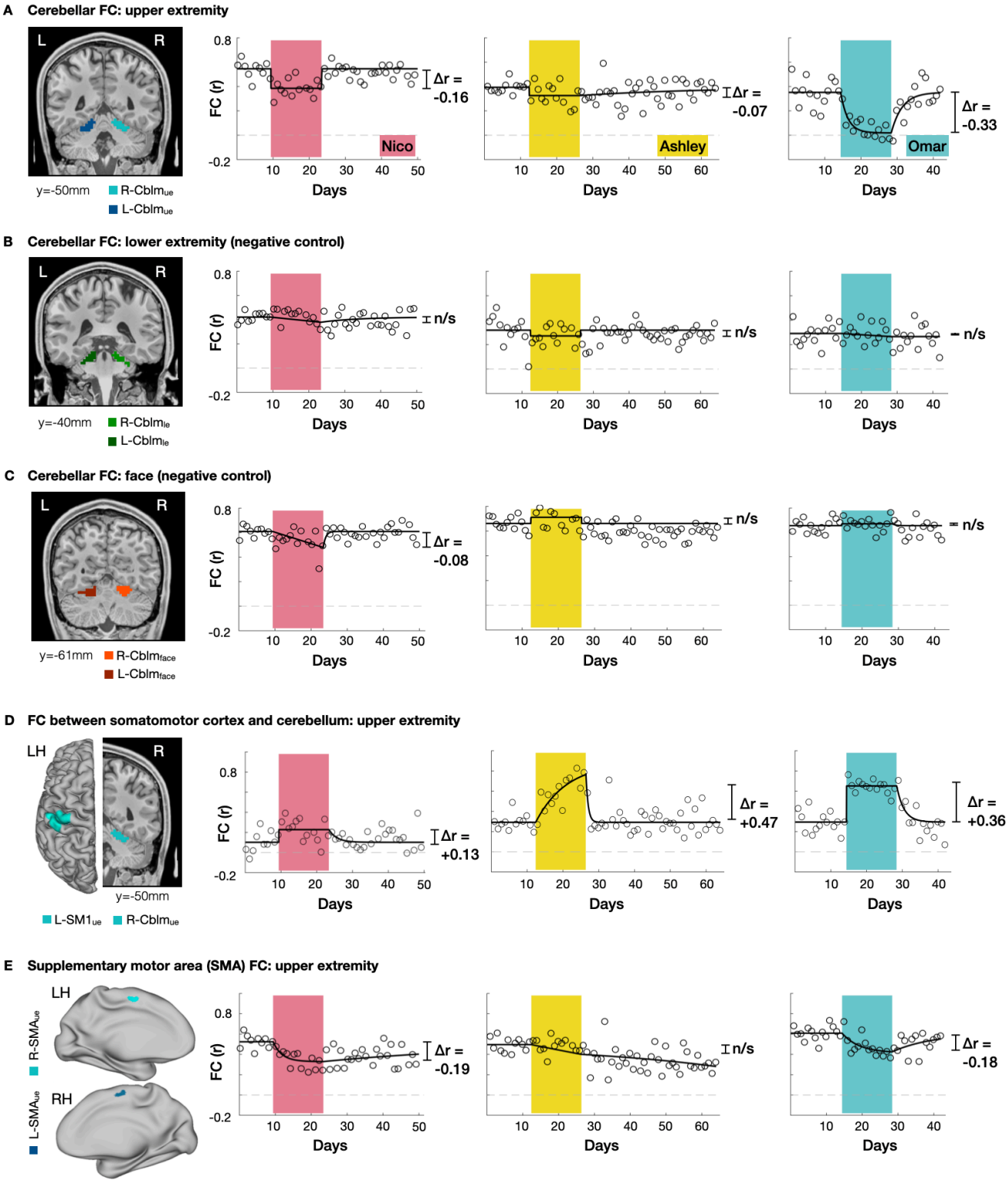

Figure S2: See next page for caption.

Figure S2: Disuse-driven changes in somatomotor functional connectivity (FC) outside of the primary somatomotor cortex, related to Figure 2. (A) *Left:* Left and right upper-extremity cerebellum (L-Cblm$_{ue}$ and R-Cblm$_{ue}$) regions of interest (ROIs), located by a hand-movement task. *Right:* Daily time course of FC between L-Cblm$_{ue}$ and R-Cblm$_{ue}$ for each participant. Δr values based on a time-varying exponential decay model (black lines, $\mathrm{dr}/dt = \alpha(\mathrm{r}_{\infty} - \mathrm{r})$). All participants showed significantly decreased FC during the cast period (Nico: Δr = -0.16, P = 0.002; Ashley: Δr = -0.07, P = 0.035; Omar: Δr = -0.33, P < 0.001). (B) *Left:* L-Cblm$_{le}$ and R-Cblm$_{le}$ ROIs, located by a foot-movement task. *Right:* Daily time course of FC between L-Cblm$_{le}$ and R-Cblm$_{le}$ for each participant. No participants showed significantly decreased FC during the cast period. (C) *Left:* L-Cblm$_{face}$ and R-Cblm$_{face}$ ROIs, located by a tongue-movement task. *Right:* Daily time course of FC between L-Cblm$_{face}$ and R-Cblm$_{face}$ for each participant. One participant showed significantly decreased FC during the cast period (Nico: Δr = -0.08, P = 0.027; Ashley: Δr = +0.05, P = 0.28; Omar: Δr = +0.02, P = 0.73). (D) *Left*: L-SM1$_{ue}$ and R-Cblm$_{ue}$ ROIs. *Right:* Daily time course of FC between L-SM1$_{ue}$ and R-Cblm$_{ue}$ for each participant. All participants showed significantly increased FC during the cast period (Nico: Δr = +0.13, P = 0.019; Ashley: Δr = +0.47, P < 0.001; Omar: Δr = +0.36, P < 0.001). (E) *Left*: L-SMA$_{ue}$ and R-SMA$_{ue}$ ROIs. *Right:* Daily time course of FC between L-SMA$_{ue}$ and R-SMA$_{ue}$ for each participant. Two participants showed significantly decreased FC during the cast period (Nico: Δr = -0.19, P < 0.001; Ashley: Δr = -0.09, P = 0.17; Omar: Δr = -0.18, P < 0.001). In total, three sets of regions were tested for FC decreases (SM1, Cblm and SMA), so a Benjamini-Hochberg correction was used to maintain a false discovery rate < 0.05. All significant effects survived correction except for the decrease in FC between L-Cblm$_{ue}$ and R-Cblm$_{ue}$ observed in one participant (Ashley, panel A).

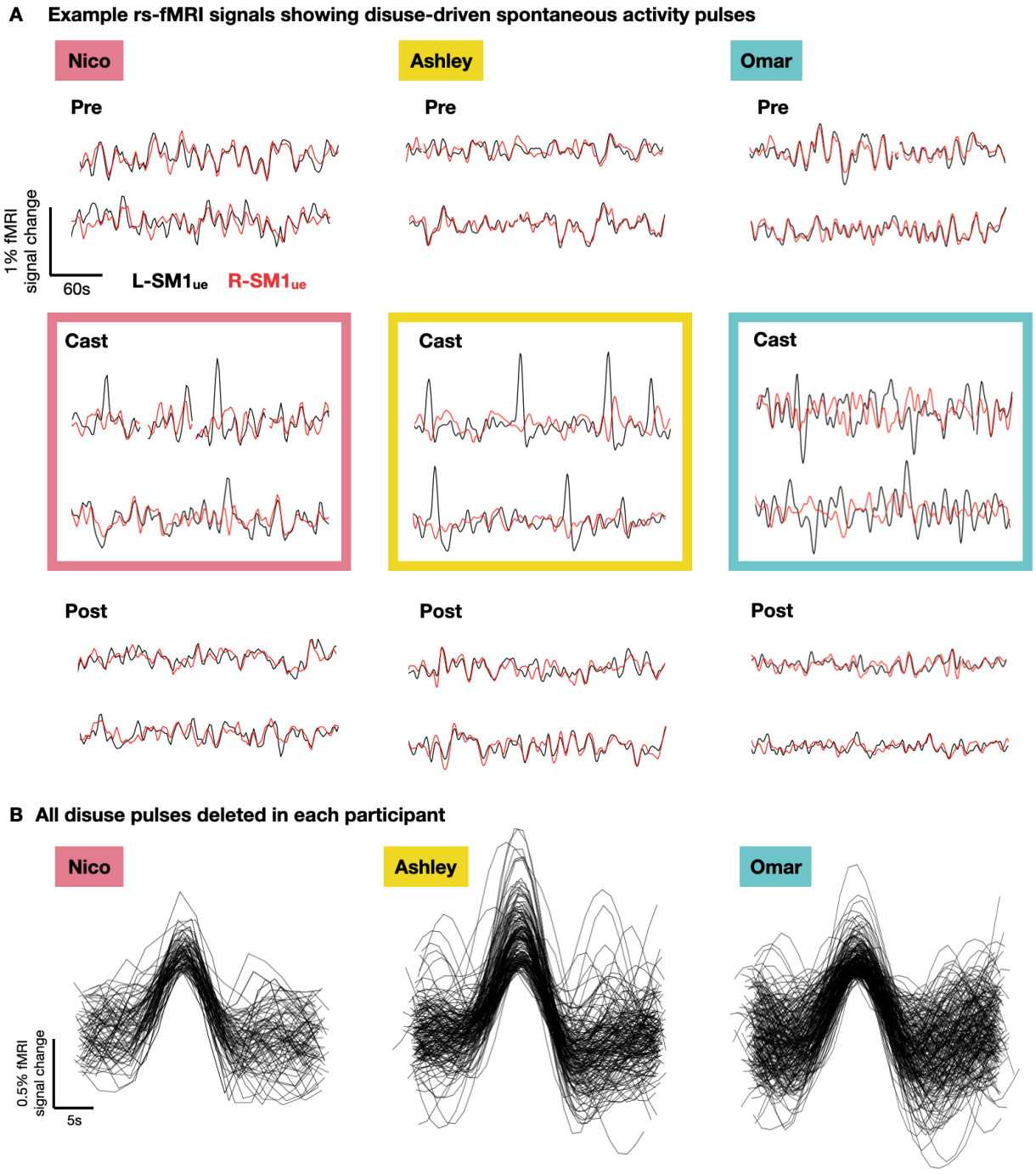

Figure S3: Example pulses in all participants, related to Figure 5. (A) Example resting-state fMRI signals from L-SM1$_{ue}$ and R-SM1$_{ue}$ during the Pre, Cast and Post periods. (B) All detected pulses superimposed on one another for each participant (Nico: n = 65; Ashley: n=144; Omar: n = 157)

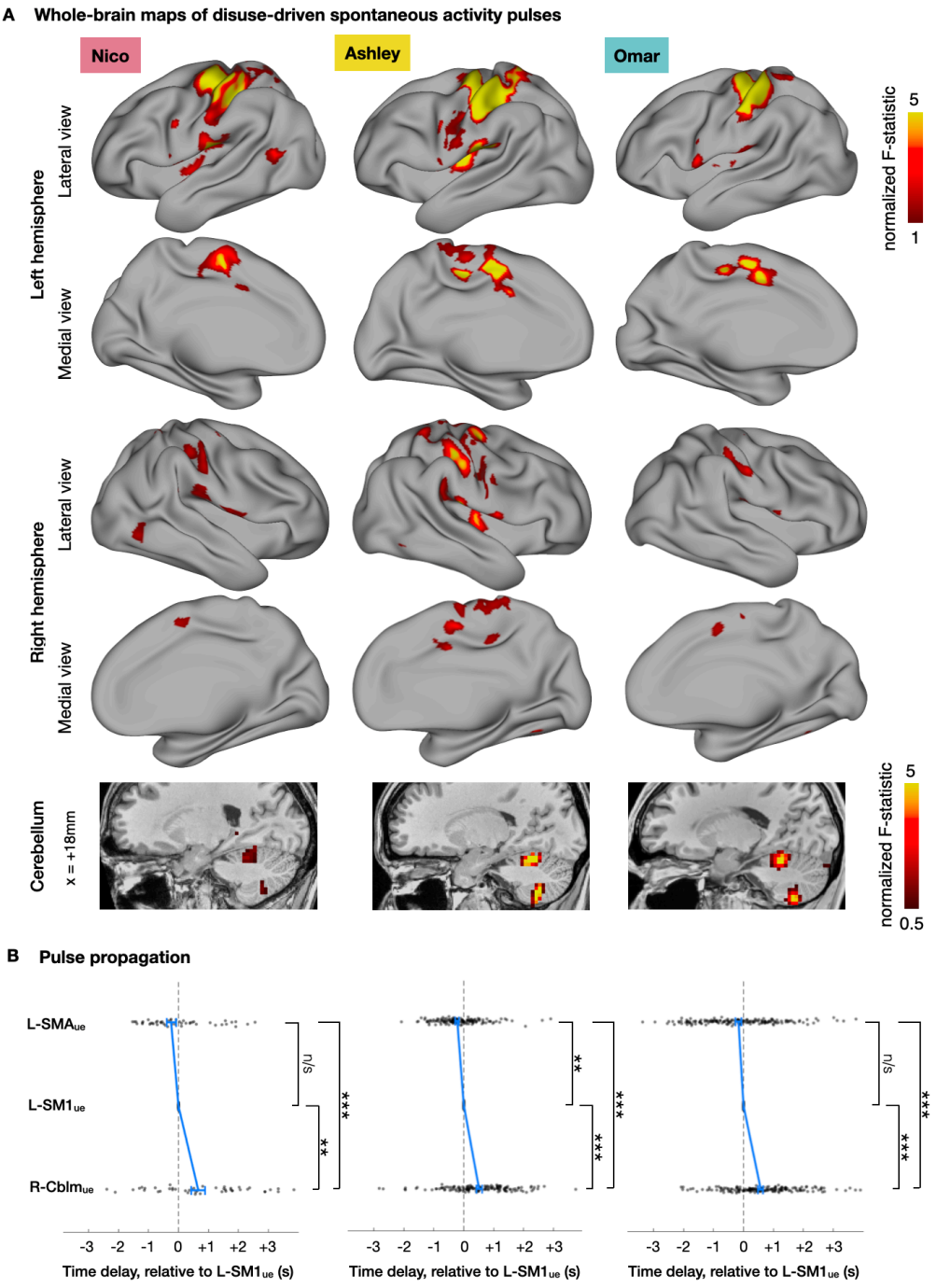

Figure S4: Whole-brain maps of disuse pulses and propagation between brain regions, related to Figure 6. (A) All participants showed spontaneous activity pulses in the left supplementary motor area, bilateral insula, right post-central sulcus and right cerebellum. Pulses were mapped using an analysis of variance (ANOVA). Since the ANOVA F-statistic increases with increasing sample sizes, we divided F-statistics by the square root of n (# of pulses) to normalize maps across participants. (B) Timing of pulses in L-SM1$_{ue}$, L-SMA$_{ue}$, and R-Cblm$_{ue}$ relative to the L-SM1$_{ue}$. Blue lines indicate median ± s.e.m. timing in each region. Time delays between regions were tested using a Wilcoxon signed rank test. **P < 0.01; ***P < 0.001. All participants showed significant time delays between L-SMA$_{ue}$ and R-Cblm$_{ue}$ (Nico: 1.1s, P < 0.001; Ashley: 0.7s, P < 0.001; Omar: 0.7s, P < 0.001) and between L-SM1$_{ue}$ and R-Cblm$_{ue}$ (Nico: 0.7s, P < 0.01; Ashley: 0.5s, P < 0.001; Omar: 0.6s, P < 0.001). Time delays between L-SMA$_{ue}$ and L-SM1$_{ue}$ were 0.2s for all participants, but this delay was only statistically significant for participant Ashley (P < 0.01). Since three time delays were tested (L-SM1$_{ue}$→R-Cblm$_{ue}$, L-SMA$_{ue}$→L-SM1$_{ue}$ and L-SMA$_{ue}$→R-Cblm$_{ue}$), a Benjamini-Hochberg correction was used to maintain a false discovery rate < 0.05. All effects survived correction.

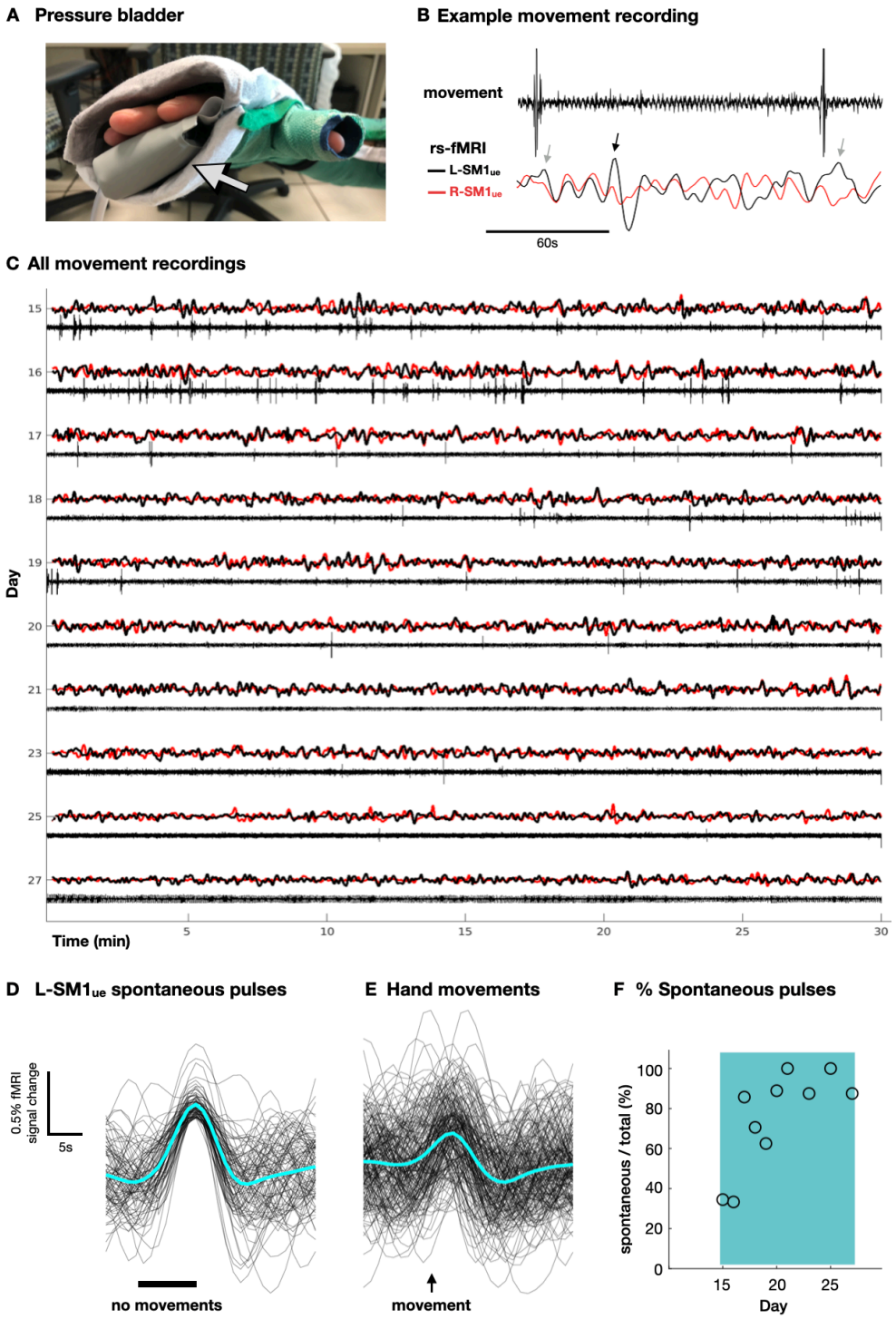

Figure S5: Pulses in L-SM1$_{ue}$ occur in the absence of hand movements, related to STAR Methods**.** (A) Hand movements in one participant (Omar) were monitored using a highly sensitive pressure bladder (gray arrow) inserted into the end of the cast. (B) Example recording from pressure bladder, plotted with rs-fMRI signals from L-SM1$_{ue}$ and R-SM1$_{ue}$. Small positive deflections in the L-SM1$_{ue}$ signal peak ~5 seconds after two hand movements (gray arrows). One spontaneous pulse in L-SM1$_{ue}$ is also shown, which occurs in the absence of hand movement (black arrow). (C) Full 30-minute recordings from 10 sessions acquired during the cast period. (D) L-SM1$_{ue}$ fMRI traces during all spontaneous pulses (pulses for which no movements were detected within 8 seconds prior to the pulse peak; n = 94). Mean pulse shown in cyan. (E) L-SM1$_{ue}$ fMRI traces surrounding each detected movement (n = 202). Peak responses occur an average of ~3 seconds after each movement. (F) Percent of all pulses detected that occurred spontaneously during each session. In total, 66% of detected pulses occurred spontaneously.

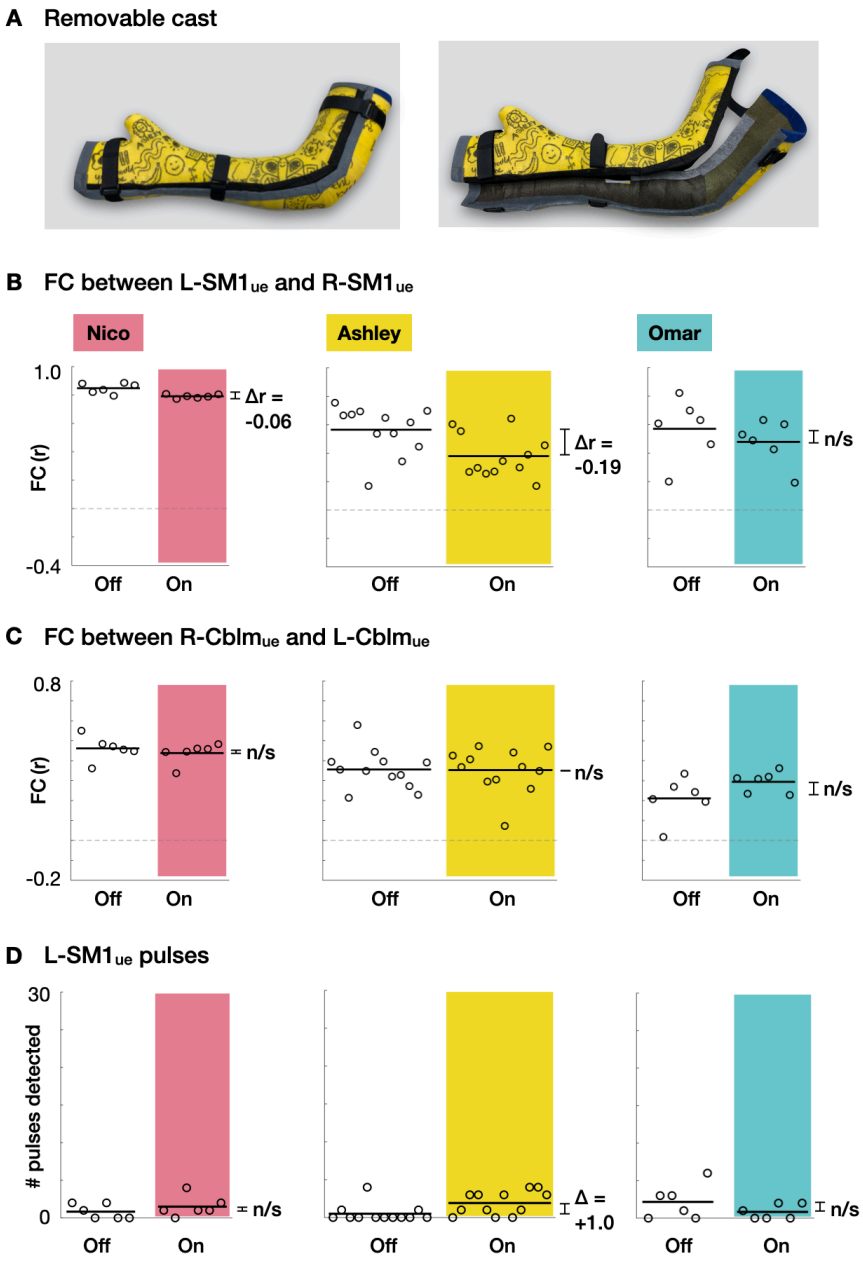

Figure S6: Wearing a cast during scanning does not recreate the effects of prolonged casting, related to STAR Methods. To separate the effects of disuse from any possible effects of wearing a cast during scans, we collected 12-24 additional scans in each participant. During half of these scans, participants wore a removable cast, constructed from casts used in the original experiment. (A) Photographs of a removable cast. (B) Functional connectivity (FC) between L-SM1$_{ue}$ and R-SM1$_{ue}$ during each session of the control experiment. Sessions are grouped into two experimental condition: wearing a removable cast ("On") and not wearing a cast ("Off"). Black lines indicate mean across sessions in each condition. Two participants showed a significant reduction in FC in the On condition relative to the Off condition, but these effects were much smaller than those observed during continuous casting (Nico: Δr = -0.06, P = 0.005; Ashley: Δr = -0.19, P = 0.01). The third participant did not show any change in FC (Omar: Δr = -0.09, P = 0.42). (C) FC between L-Cblm$_{ue}$ and R-Cblm$_{ue}$ was not significantly different during On sessions compared to Off sessions in any participant (Nico: Δr = -0.02, P = 0.49; Ashley: Δr = 0.00, P = 0.94; Omar: Δr = +0.08, P = 0.12). (D) Number of pulses detected during each scan of the Off and On conditions, plotted on the same axes as Figure 5C. Very few events were detected in all participants. In one participant, significantly more events were detected in the ON condition (Ashley: mean pulse count = 0.5 OFF vs. 1.5 ON, t = +2.5, P = 0.02). The remaining two participants did not show a significant difference between conditions (Nico: mean pulse count = 0.8 OFF vs. 1.5 ON, t = +0.96, P = 0.36; Omar: 2.2 OFF vs. 0.8 ON, t = -1.3, P = 0.22).

Supplementary Table 1: MRI acquisition and processing parameters, related to STAR Methods.

	Nico	**Ashley**	**Omar**
Age (years)	35	25	27
Sex	Male	Female	Male
Handedness (Edinburgh Inventory)	Right-handed (+100)	Right-handed (+91)	Right-handed (+60)
Scan time	5:00am	9:00pm	9:00pm
Scanner	Siemens Trio 3T	Siemens Prisma 3T	Siemens Prisma 3T
T1 sequence			
Pulse sequence type	Gradient echo	Gradient echo	Gradient echo
Image type	3D MP-RAGE	3D MP-RAGE	3D MP-RAGE
Field of view (mm)	204.8x204.8x179.2	240x240x166.4	240x240x166.4
Orientation	Sagittal	Sagittal	Sagittal
TE (ms)	3.74	2.22	2.22
TR (ms)	2400	2400	2400
TI (ms)	1000	1000	1000
Flip angle (°)	8	8	8
Matrix size	256x256x224	300x320x208	300x320x208
Slice thickness (mm)	0.8	0.8	0.8
Voxel size (mm)	0.8 x 0.8 x 0.8	0.8 x 0.8 x 0.8	0.8 x 0.8 x 0.8
T2 sequence			
Pulse sequence type	Spin echo	Spin echo	Spin echo
Image type	3D T2-SPC	3D T2-SPC	3D T2-SPC
Field of view (mm)	204.8x204.8x179.2	204.8x204.8x179.2	204.8x204.8x179.2
Orientation	Sagittal	Sagittal	Sagittal
TE (ms)	479	563	563
TR (ms)	3200	3200	3200
Flip angle (°)	120	120	120
Matrix size	256x256x224	300x320x208	300x320x208
Slice thickness (mm)	0.8	0.8	0.8
Voxel size (mm)	0.8 x 0.8 x 0.8	0.8 x 0.8 x 0.8	0.8 x 0.8 x 0.8
BOLD sequence			
Pulse sequence type	2D Gradient echo	2D Gradient echo	2D Gradient echo
Image type	Echo planar	Echo planar	Echo planar
Field of view (mm)	256x256x144	234x234x145.6	234x234x145.6
Multi-band factor	1	4	4
TE (ms)	27	33	33
TR (ms)	2200	1100	1100
Flip angle (°)	90	84	84
Matrix size	64x64x36	90x90x56	90x90x56
Slice thickness (mm)	4	2.6	2.6
Voxel size (mm)	4 x 4 x 4	2.6 x 2.6 x 2.6	2.6 x 2.6 x 2.6
FD threshold (mm)	0.2	0.1	0.1
DVARS threshold (% rms)	6	6	6